31st Annual International Conference of the IEEE EMBS
Minneapolis, Minnesota, USA, September 2-6, 2009

Elastic Nonlinearity Imaging

Timothy J. Hall*, Assad A. Oberai†, Paul E. Barbone‡, Amy M. Sommer*, Nachiket H. Gokhale‡, Sevan Goenezen† and Jingfeng Jiang*
*Medical Physics Department, University of Wisconsin, Madison, Wisconsin 53706 Email: tjhall@wisc.edu
†Mechanical Aerospace and Nuclear Engineering, Rensselaer Polytechnic Institute, Troy, NY 12180
‡Department of Aerospace and Mechanical Engineering, Boston University, Boston, MA 02215

***Abstract*—Previous work has demonstrated improved diagnostic performance of highly trained breast radiologists when provided with B-mode plus elastography images over B-mode images alone. In those studies we have observed that elasticity imaging can be difficult to perform if there is substantial motion of tissue out of the image plane. So we are extending our methods to $3D$/$4D$ elasticity imaging with $2D$ arrays. Further, we have also documented the fact that some breast tumors change contrast with increasing deformation and those observations are consistent with *in vitro* tissue measurements. Hence, we are investigating imaging tissue stress-strain nonlinearity. These studies will require relatively large tissue deformations (e.g., $>$ 20%) which will induce out of plane motion further justifying $3D$/$4D$ motion tracking. To further enhance our efforts, we have begun testing the ability to perform modulus reconstructions (absolute elastic parameter) imaging of *in vivo* breast tissues. The reconstructions are based on high quality $2D$ displacement estimates from strain imaging. Piecewise linear (secant) modulus reconstructions demonstrate the changes in elasticity image contrast seen in strain images but, unlike the strain images, the contrast in the modulus images approximates the absolute modulus contrast. Nonlinear reconstructions assume a reasonable approximation to the underlying constitutive relations for the tissue and provide images of the (near) zero-strain shear modulus and a nonlinearity parameter that describes the rate of tissue stiffening with increased deformation. Limited data from clinical trials are consistent with *in vitro* measurements of elastic properties of tissue samples and suggest that the nonlinearity of invasive ductal carcinoma exceeds that of fibroadenoma and might be useful for improving diagnostic specificity. This work is being extended to $3D$.**

I. Introduction

Early detection has improved the prognosis for breast cancer diagnosis. But biopsy, the gold standard for diagnosis, returns a benign diagnosis approximately 70% of the time. Biopsy would be performed on fewer benign lesions if diagnostic confidence was higher following noninvasive imaging techniques. Elastography has been proposed as an adjunct to the cohort of technologies available to increase diagnostic accuracy and increase clinicians confidence.

Attention in elastography research is typically dedicated to imaging contrast in linear (small incremental strain) stiffness. Most soft tissues, however, tend to stiffen with increasing applied strain. This phenomenon is usually represented by a nonlinear relation between stress and strain. *In vitro* measurements [1], [2] indicate that fibroadenoma (FA) and invasive ductal carcinoma (IDC) have similar linear (small strain) elastic properties, but significantly different nonlinear elastic properties (see fig. 1). Furthermore, of all breast tissues measured, DCIS has the greatest nonlinear behavior [1]. These data imply that there is considerable untapped diagnostic potential in examining the nonlinear elastic properties of soft tissues.

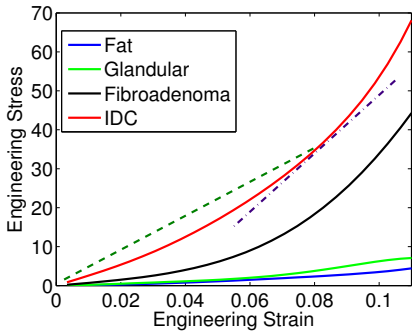

Fig. 1: A plot of the stress-strain relationship of various breast tissues adapted from [2]. The dashed green and dot-dash blue lines show the secant and tangent modulus of IDC at 8% strain, respectively. For sufficiently large strains estimates of either the secant modulus or the small-strain modulus and nonlinearity should be unique among tissue types whereas the tangent modulus at unknown local strain might not be unique.

A nonlinear stress-strain response in breast tissues can conceivably be observed in at least three ways. Perhaps the simplest is to observe a change in strain contrast with increasing applied strain [3]. The next, in order of complexity, is to use a quasi-linear modulus reconstruction. In this case, an effective shear modulus is reconstructed at each level of applied strain. The third way is to assume that the stress-strain law for tissue follows a particular functional form, and then to reconstruct the stiffening parameter that appears in that form. Although each of these has relative advantages and disadvantages, quantitative modulus imaging likely reduces ambiguities observed in relative strain images and conveys additional information not otherwise available.

This work compares the deformation-dependent strain image contrast with quasi-linear (secant) modulus reconstructions and nonlinear modulus reconstruction. These methods were tested on a small group (to date) of five fibroadenoma (benign) and five invasive ductal carcinoma (malignant) tumors.

At least two other research groups have taken steps to ex-

ploit the potential of nonlinear elasticity imaging. Skovoroda and coworkers made great progress in this direction a few years ago [4]–[6]. They focused largely on studying changes in strain contrast with overall applied strain. Quantitative reconstruction is addressed in [4]. This treatment accounts for large deformation, but assumes a linear (neoHookean) stress-strain law. Nitta and Shiina [7], on the other hand, present "nonlinear elasticity" images that show tissue nonlinear stiffening. These represent the slope of the Young's modulus with strain, based on two assumptions: stress is uniaxial and constant, and the stress-strain law is quadratic. Thus their images may be thought of as rescaled strain-slope images. The methods we've employed [8], [9] go significantly beyond these earlier studies in terms of the objective modeling of tissue mechanics, the inversion methods, and particularly the application to clinical data.

We are extending this work to $3D$ through the use of novel $2D$ array transducers and commercially available mechanically rocked $1D$ arrays (MRA) for $3D$/$4D$ data acquisition. Preliminary results for linear $3D$ reconstructions are very encouraging. That work is being extended through the development of phantoms with nonlinear stress-strain behavior in both the background and spherical inclusion.

II. Methods

The $2D$/$3D$ (time being the 3rd dimension) radio frequency (RF) echo data from a Siemens Elegra or Antares was recorded during real-time freehand elasticity imaging of patients scheduled for breast biopsy. A $1D$ linear array (VFX13-5) was used which provides $2D$ displacement and strain fields. The data included in this study is a subset of that from previous studies of elasticity imaging [3], [10] and all pathology was biopsy-confirmed. The study was approved by the appropriate institutional review boards and each subject provided informed consent.

Five cases of fibroadenoma and five invasive ductal carcinoma were selected from archived data sets. Cases were selected on the basis of high quality displacement estimates (assessed using an objective measure of displacement estimate accuracy [11]) with at least 10% accumulated axial strain during application of compressive force (for consistency among data). Displacement estimate accuracy is sufficient to form consistent strain images over at least 10% axial strain [12]. Displacement and strain were estimated with a predictive search block matching algorithm that employs lateral guidance [13]. The algorithm devotes a significant fraction of its computational time to obtaining a reliable estimate of the displacement along the central RF echo line in the data field. That displacement estimate is then used to guide motion tracking estimates and limit the search region (predict motion) for laterally adjacent RF echo lines of data. The algorithm can be naturally split into two parallel processes to reduce computational time.

The $3D$/$4D$ (time being the 4th dimension) RF echo data from a Siemens Antares while the transducer was securely held with a fixture. RF echo data was acquired from a 100mm$\times$100mm$\times$70mm (tall) oil-in-gelatin phantom that contained a 10mm diameter spherical inclusion five times stiffer than the background (but lacked B-mode contrast) using either a 4MHz C7F2 MRA or a prototype 10MHz $2D$ array cMUT [14].

A. Modulus Reconstruction

It is common in tissue elasticity imaging to assume that the relative strain distribution is representative of the relative shear (or Young's) modulus distribution. However, this assumption is only valid if uniaxial stress conditions are closely approximated. "Elastic Modulus Imaging" or "Biomechanical Imaging," to distinguish it from strain imaging, provides quantitative estimates of tissue mechanical properties from measured displacement and/or strain fields by formulating an inverse problem in terms of an assumed constitutive law and the measured displacement (and/or strain) fields as the inputs. This inverse problem is formulated and solved as an optimization problem: determine the elastic modulus distribution that when used in a forward solver for the displacement field, gives the best match to the observed displacement fields. Figure 2 illustrates the approach to iterative modulus reconstruction.

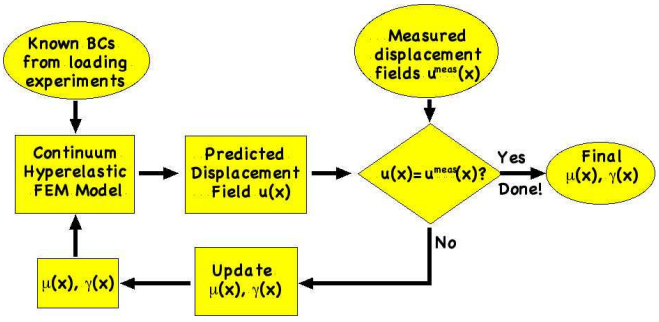

Fig. 2: A flowchart of the nonlinear modulus reconstruction algorithm.

The resolution requirements in medical imaging applications drive the computational size of the problem, which can be large. The fully nonlinear optimization problem involves $O(10^4)$ optimization variables. The efficient solution of this problem requires an efficient gradient based optimization method, an efficient technique to repeatedly evaluate the functional, and an efficient evaluation of the gradient. For a gradient based optimization method, we use a BFGS quasi-Newton method [15]. We use the adjoint method to evaluate the gradient efficiently [16], [17]. Once the functional is evaluated, the adjoint method requires only one linear solve to evaluate the gradient, even for the nonlinear elasticity problem. In the nonlinear elastic inverse problem, the cost is dominated by evaluating the forward solution at each property update. We manage this cost by using a novel continuation strategy in the material property distribution. The net result is that the cost of solving the nonlinear

inverse problem is only about two times that of solving the corresponding forward problem.

III. Results

Figure 3 shows side by side B-mode and corresponding strain images, under small strain 3(a) and high strain 3(b) of a fibroadenoma. The strain contrast of the fibroadenoma at higher strain is lower than at smaller strain. This is most likely due to the background tissue becoming stiffer with applied strain faster than the fibroadenoma stiffens with overall applied strain. In part, this may be expected since the stiff fibroadenoma experiences relatively low overall strain, in contrast to the normal background tissue. This change in relative stiffness between the fibroadenoma and background normal tissue is reflected in the secant modulus images (c.f. fig 1). These images clearly show the fibroadenoma softening relative to the background with increased applied strain. Note that the secant modulus reconstructions are made with the top few ($\approx$10) displacement estimates excluded to improve stability of the reconstruction.

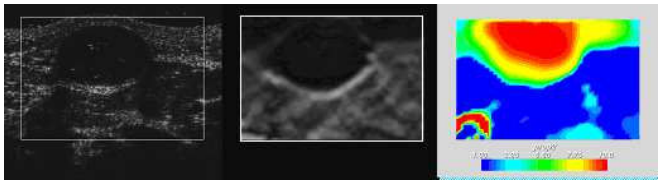

(a) Minimal preloading

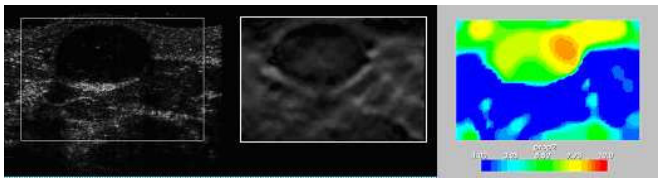

(b) 12% overall applied strain

Fig. 3: B-mode, 1% incremental strain and secant modulus images of fibroadenoma.

Figure 4 shows the corresponding images for an invasive ductal carcinoma (IDC). Unlike the fibroadenoma, the strain contrast of the IDC increases at higher strain compared to lower strain. The stiffening that is implied by the change in strain contrast is confirmed in the secant modulus images. Together, these show that, relative to the background, the IDC is stiffening with applied strain.

Both the strain images and the secant modulus reconstruction images can be displayed in a sequence (e.g., a movie loop) to demonstrate whether these changes are occurring as a smooth transition or the observed changes are more likely due to noise.

A. Summary Images of Hyperelastic Mechanical Properties

The same data that were used to produce the strain images shown in figs 3 and 4 can be used to reconstruct the nonlinear elastic properties, μ (the near-zero strain shear modulus)

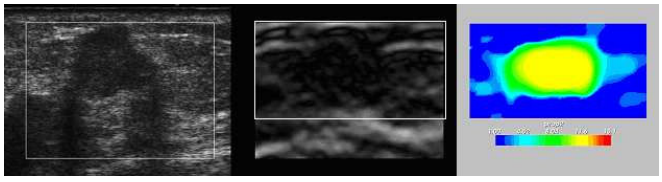

(a) Minimal preloading

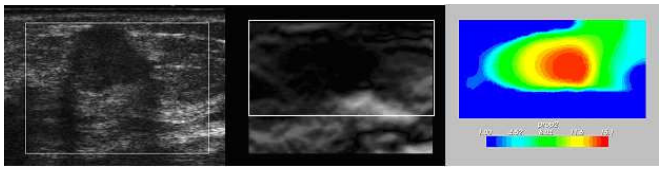

(b) 11% overall applied strain

Fig. 4: B-mode, 1% incremental strain and secant modulus images of invasive ductal carcinoma.

and γ (the nonlinearity parameter). Results are shown in fig. 5. The model [18] assumes an exponential increase in the stiffness with strain, with γ in the exponent. Note that the shear moduli μ are in general agreement with those depicted in fig 3 and 4. The fact that the fibroadenoma is nearly invisible in the γ image implies that this fibroadenoma and background normal tissue stiffen at approximately the same rate. Note the strong contrast of the IDC in the γ image, in particular in its core. The nonlinear stiffening is clearly different for the IDC compared to the fibroadenoma.

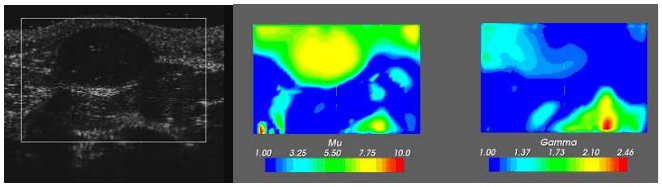

(a) (b)

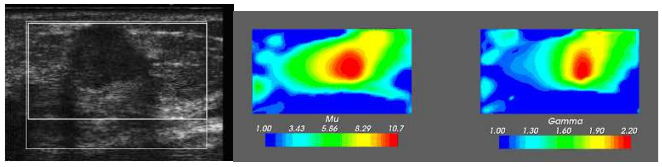

(c) (d)

Fig. 5: B-mode and nonlinear modulus reconstructions for a fibroadenoma (top row) and an invasive ductal carcinoma (bottom row). Left: B-mode for reference. Center: Linear (small strain) shear modulus reconstructed as part of the full nonlinear elastic reconstruction. Right: The nonlinear stiffening parameter, γ, as it appears in the Veronda-Westman constitutive model.

One difficulty with imaging elastic nonlinearity is the need for sufficiently large deformation to detect a deviation from linear response. Although the accumulated frame-average strain in each case studied here exceeded about 10% axial

strain, the deformation in the background typically exceeded 12% axial strain but the strain in the segmented lesion was below about 4%. This small total strain in the lesion is marginal for estimating elastic nonlinearity. Larger deformations are required to confidently estimate elastic nonlinearity. Two-dimensional tracking with $1D$ arrays limits the ability to track large *in vivo* tissue deformations to approximately 10% axial strain. Extending these techniques to $3D/4D$D tracking in volume data fields will allow tracking much larger deformations with increased accuracy. This preliminary data suggests that tracking at least 15% axial strain is required to obtain sufficiently large deformation in the lesion to estimate the nonlinearity parameter with confidence.

Initial studies of $3D/4D$ tracking in phantoms is very encouraging. Figure 6a shows a $3D$ image of the relative strain in the phantom with a 10mm diameter spherical inclusion. White is mapped to 3.5% strain. A linear $3D$ reconstruction of the shear modulus distribution based on the same displacement data is shown in Figure 6b. High CNR is observed in both the strain image and modulus image. Further, the modulus contrast is in excellent agreement with those measured independently for the constituent phantom materials.

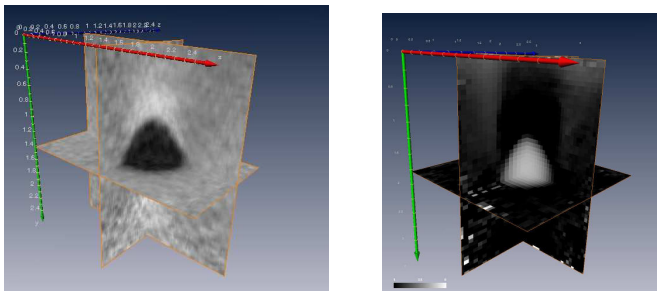

(a) (b)

Fig. 6: $3D$ strain (a) and secant modulus images (b) of a phantom containing a spherical inclusion.

Another difficulty in this work is the need for data to include RF acquisition with minimal contact with the skin surface (near zero surface pressure). It is essential to include this data within the sequence of displacement (or strain) fields in a nonlinear reconstruction to adequately estimate the small strain shear modulus. Further, a force sensor (or preferably a pressure sensor array) is necessary to measure the applied force (or pressure distribution) to obtain absolute elastic modulus images (instead of relative modulus images).

IV. Conclusions

Current $2D$ tracking with data from $1D$ array transducers limits accurate motion tracking to about 10% axial strain. That deformation is sufficient to demonstrate differences in the secant modulus but is marginally sufficient to demonstrate differences in the elastic nonlinearity of various breast tissue types. The results are consistent with *in vitro* tissue studies and the observations of deformation-dependent strain image contrast, but provide a quantitative measure of *in vivo* tissue elastic nonlinearity that might help improve classification of tumor types in a larger study.

V. Acknowledgements

We are grateful to Bill Svensson (Charing Cross Hospital, London, UK) and Nick Hangiandreou and Gina Hesley (Mayo Clinic, Rochester, MN) for their assistance in acquiring the data for this study. This work was supported in part with funding from NIH grants R01CA100373 (TJH), R21CA133488 (TJH) and the NFS (PEB).

References

[1] T. A. Krouskop, T. Wheeler, F. Kallel, and T. Hall, "The elastic moduli of breast and prostate tissues under compression," *Ultrasonic Imaging*, vol. 20, pp. 260–274, 1998.

[2] P. S. Wellman, E. P. Dalton, D. Krag, K. A. Kern, and R. D. Howe, "Tactile imaging of breast masses," *Arch Surg*, vol. 136, pp. 204–208, 2001.

[3] T. J. Hall, Y. Zhu, and C. S. Spalding, "In vivo real-time freehand palpation imaging," *Ultrasound Med Biol*, vol. 29, no. 3, pp. 427–435, 2002.

[4] A. R. Skovoroda, M. A. Lubinski, S. Y. Emelianov, and M. O'Donnell, "Reconstructive elasticity imaging for large deformations," *IEEE Trans Ultrason, Ferroelec, Freq Cont*, vol. 46, no. 3, pp. 523–535, 1999.

[5] R. Erkamp, S. Y. Emelianov, A. R. Skovoroda, and M. O'Donnell, "Nonlinear elasticity imaging," in *IEEE Ultrason. Symp. Proc.*, 2002, pp. 1891–1894.

[6] ——, "Nonlinear elasticity imaging: Theory and phantom study," *IEEE Trans Ultrason, Ferroelec, Freq Cont*, vol. 51, no. 5, pp. 532–539, 2004.

[7] N. Nitta and T. Shiina, "A visualization of nonlinear elasticity property of tissues by ultrasound," *Electronics and Communications in Japan Part III-Fundamental Electronic Science*, vol. 85, no. 12, pp. 9–18, 2002.

[8] N. H. Gokhale, "Nonlinear elasticity imaging using the adjoint method," Ph.D., Boston University, 2007.

[9] M. Richards, "Quantitative three-dimensional elasticity imaging," Ph.D., Boston University, 2007.

[10] E. S. Burnside, T. J. Hall, A. M. Sommer, G. K. Hesley, G. A. Sisney, W. E. Svensson, and N. J. Hangiandreou, "Ultrasound strain imaging to improve the decision to biopsy solid breast masses," *Radiology*, vol. 245, no. 2, pp. 401–410, 2007.

[11] J. Jiang, T. J. Hall, and A. M. Sommer, "A novel performance descriptor for ultrasonic strain imaging: A preliminary study," *IEEE Trans Ultrason, Ferroelec, Freq Cont*, vol. 53, no. 6, pp. 1088–1102, 2006.

[12] A. M. Sommer, T. J. Hall, and J. F. Jiang, "Strain image contrast for differentiating in vivo breast lesions," in *IEEE Ultrason. Symp. Proc.*, 2006, pp. 2052–2055.

[13] J. Jiang and T. J. Hall, "A parallelizable real-time motion tracking algorithm with applications to ultrasonic strain imaging," *Physics in Medicine and Biology*, vol. 52, no. 13, pp. 3773–3790, 2007.

[14] C. Daft, P. Wagner, S. Panda, and I. Ladabaum, "Elevation beam profile control with bias polarity patterns applied to microfabricated ultrasound transducers," in *Proc. IEEE Ultrasonics Symposium*, 2003, pp. 1578–1581.

[15] J. Nocedal and S. Wright, *Numerical Optimization*. New York: Springer, 1999.

[16] A. A. Oberai, N. H. Gokhale, M. M. Doyley, and J. C. Bamber, "Evaluation of the adjoint equation based algorithm for elasticity imaging," *Physics Med Biol*, vol. 49, no. 13, pp. 2955–2974, 2004.

[17] A. A. Oberai, N. H. Gokhale, and G. R. Feijoo, "Solution of inverse problems in elasticity imaging using the adjoint method," *Inverse Problems*, vol. 19, no. 2, pp. 297–313, 2003.

[18] D. Veronda and R. Westman, "Mechanical characterization of skin–finite deformations," *Journal of Biomechanics*, vol. 3, no. 1, pp. 111–122, 1970.